WS_2 nanotubes as tips in scanning probe microscopy

A. Rothschild
Department of Materials and Interfaces, Weizmann Institute of Science, Rehovot 76100, Israel

S. R. Cohen
Chemical Services Unit, Weizmann Institute of Science, Rehovot 76100, Israel

R. Tenne[a)]
Department of Materials and Interfaces, Weizmann Institute of Science, Rehovot 76100, Israel

(Received 9 August 1999; accepted for publication 29 October 1999)

WS_2 nanotubes a few microns long were attached to microfabricated Si tips and tested afterwards in an atomic force microscope by imaging a ''replica'' of high aspect ratio, i.e., deep and narrow grooves. These WS_2 nanotube tips provide a considerable improvement in image quality for such structures when compared with commercial ultrasharp Si tips. The nanotube tip apex shape was extracted by blind reconstruction from an image of Ti spikes, showing a smooth cylindrical profile up to the end. © *1999 American Institute of Physics.* [S0003-6951(99)03151-4]

The synthesis of bulk quantities of WS_2 nanotubes a few microns long have been reported recently.[1] The distribution of nanotube diameters is bimodal with about 20% of the nanotubes having a diameter of about 100 nm, and the rest are 20–40 nm in diameter. Figure 1 shows a scanning electron microscopy (SEM) image of (a) a mat of WS_2 nanotubes, (b) an enlarged image of this mat, and (c) a single WS_2 nanotube micrograph, obtained by transmission electron microscopy (TEM). Many of the nanotubes grow in bundles as shown in Fig. 1(b). Among the various potential applications, the use of these nanotubes as tips for atomic force microscopy (AFM) was explored, first.

For investigating high aspect ratio features as are now common in the microelectronics industry, conventional microfabricated AFM tips are of limited use. Without special treatment (such as ion beam milling of the Si tip), aspect ratios of 3:1 or lower are typical. Thus, when scanning over high aspect ratio features, the tip profile, rather than that of the surface, is imaged. For instance, the width of such a tip at a height of 3 μm from its apex is about 1 μm compared to a uniform thickness of 20–30 nm for the WS_2 nanotubes. Based on this analysis, it was deduced that WS_2 nanotube tips should be more suitable for the analysis of deep and narrow structures than commercially available tips. In this letter, we present the performance of WS_2 nanotube tips applied to a ''replica'' sample with deep features of varied width.

Carbon nanotubes have previously been applied as AFM tips, and it appears that these tips have potential to probe extremely narrow structures,[2] because of the slenderness of the nanotubes (diameter of 1–5 nm). Furthermore, the growth of carbon nanotube tips directly onto Si cantilevers has been recently demonstrated.[3]

Details of the production and growth mechanism of the WS_2 nanotubes have been given before.[1] In short, asymmetric nanoparticles of WO_{3-x} were obtained by heating a tungsten filament in the presence of water vapor under vacuum. These nanoparticles are subsequently converted into WS_2 nanotubes by firing them in H_2S under a reducing atmosphere. The mounting of the WS_2 nanotubes on ultrasharp Si tips (NT-MTD-NSCS12 noncontact) was performed according to a published procedure,[2] consisting of first transferring glue from conductive carbon adhesive tape onto the Si tip and subsequently sticking the nanotube or a bundle of nanotubes onto this tip by touching to an area of the tape dusted with a powder of the nanotubes. The entire process is viewed under a high power (×800) inverted light microscope (Axiovert 25), and sample movement controlled by micromanipulators. In these preliminary experiments, this procedure yielded one high quality tip out of ten to twenty attempts. ''Etching'' by applying a voltage between nanotube tip and surface when they were in close proximity as applied successfully with carbon nanotube tips did not improve performance here. Some of the failed attempts can be ascribed to the fact that about 20% of the nanotubes have a large diameter (100 nm), which make them unsuitable for the present experiments. Unfortunately, the limited optical magnification, did not permit one to distinguish between a single nanotube or a bundle of nanotubes. Nonetheless, no evidence of a multiple tip was observed in the images.

In order to demonstrate the capabilities of these tips for investigating deep and narrow structures, they were used to image trenches of varying linewidth and a depth of 670 nm. As seen in Fig. 2, the WS_2 nanotube tips perform significantly better than microfabricated sharp Si tips. Indeed, while the WS_2 nanotube tip follows the contour of even the finest ''replica'' and reaches its bottom [Fig. 2(b)], the commercial Si tip is unable to do so [Fig. 2(a)]. The Si tip is also unable to follow the sample's contour very smoothly [Fig. 2(c)], since the tip surface is not passivated and strong interaction with the substrate at close proximity is therefore unavoidable. On the contrary, the WS_2 nanotube tip does not exhibit a strong affinity towards the probed surfaces, even in the intermittent contact mode applied here. Therefore, the nanotube tip does not stick to the surface during the scan and the trace is much smoother in this case [Fig. 2(d)]. This behavior is a manifestation of the passivated surface of the

a)Electronic mail: cpreshef@weizmann.weizmann.ac.il

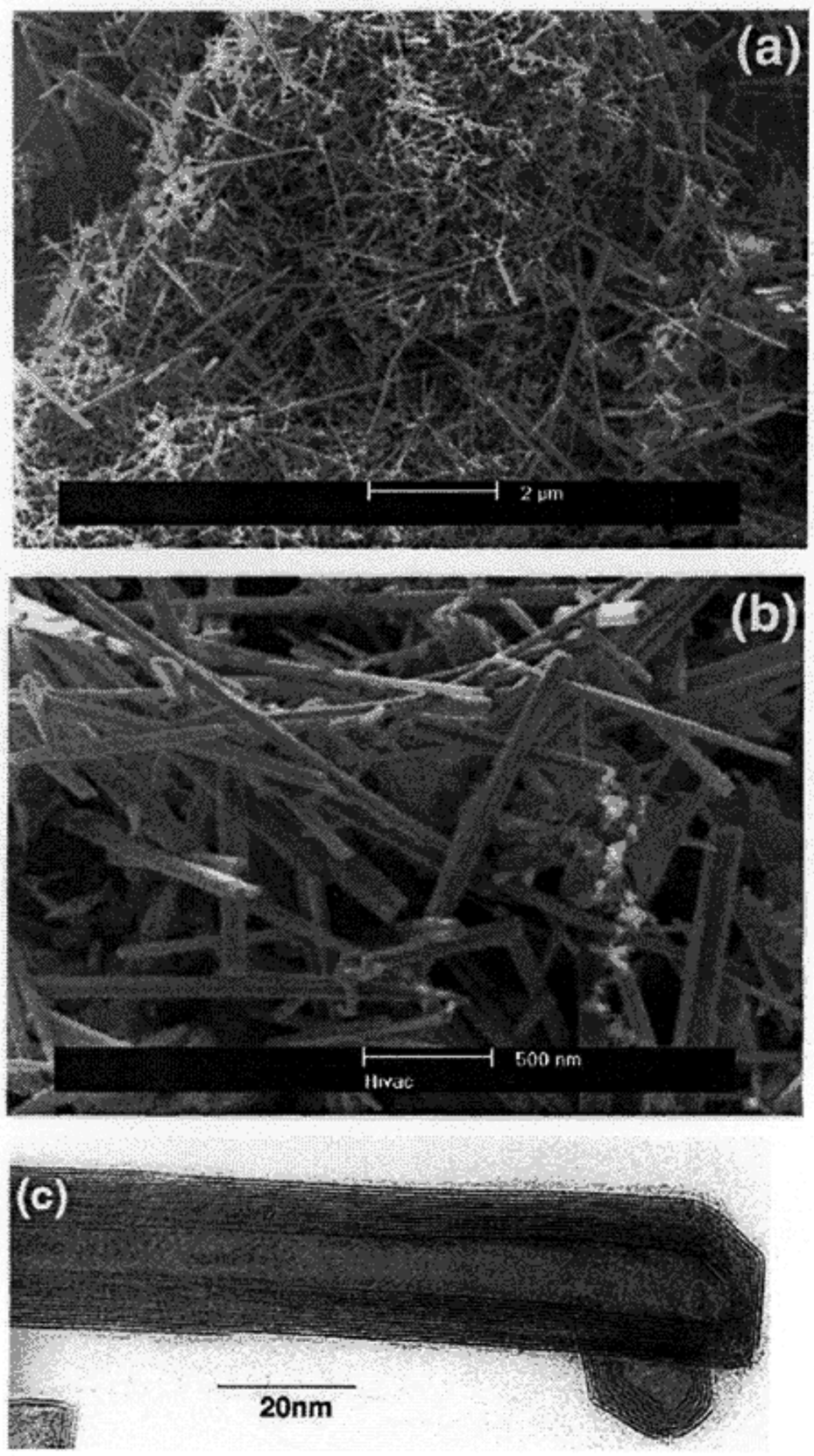

FIG. 1. Typical SEM picture of a WS_2 nanotube mat deposited on a gold surface; (d) enlargment of one portion of the previous mat; (c) TEM micrograph of a hollow multiwalled WS_2 nanotubes as they are found in the mat.

nanotube, which exhibits little affinity to the underlying surface.

Another measure for the quality of the image is the steepness of the trench edges. Comparison of the profiles obtained with the nanotube [Fig. 2(b)] and that of the Si tip [Fig. 2(a)], clearly shows the advantage of using the former.

Also remarkably, a repeated testing of this tip over a period of two months did not reveal any deterioration in the quality of the AFM image. This observation indicates that the WS_2 tip is chemically very stable and does not pick-up contaminants from the surroundings. This is another indication for the inertness of the nanotube surface, which makes it very useful for the present application.

To get an idea of the real shape of the apex tip which had scanned the sample's surface, scanning on a Ti tip calibrator[4] and subsequent blind reconstruction of the WS_2 tip shape was done (Fig. 3).[5] This process uses a deconvolution procedure, whereby the sharpest features on the image surface are used to obtain an estimate of the tip shape. An iterative procedure results in the best tip approximation. This

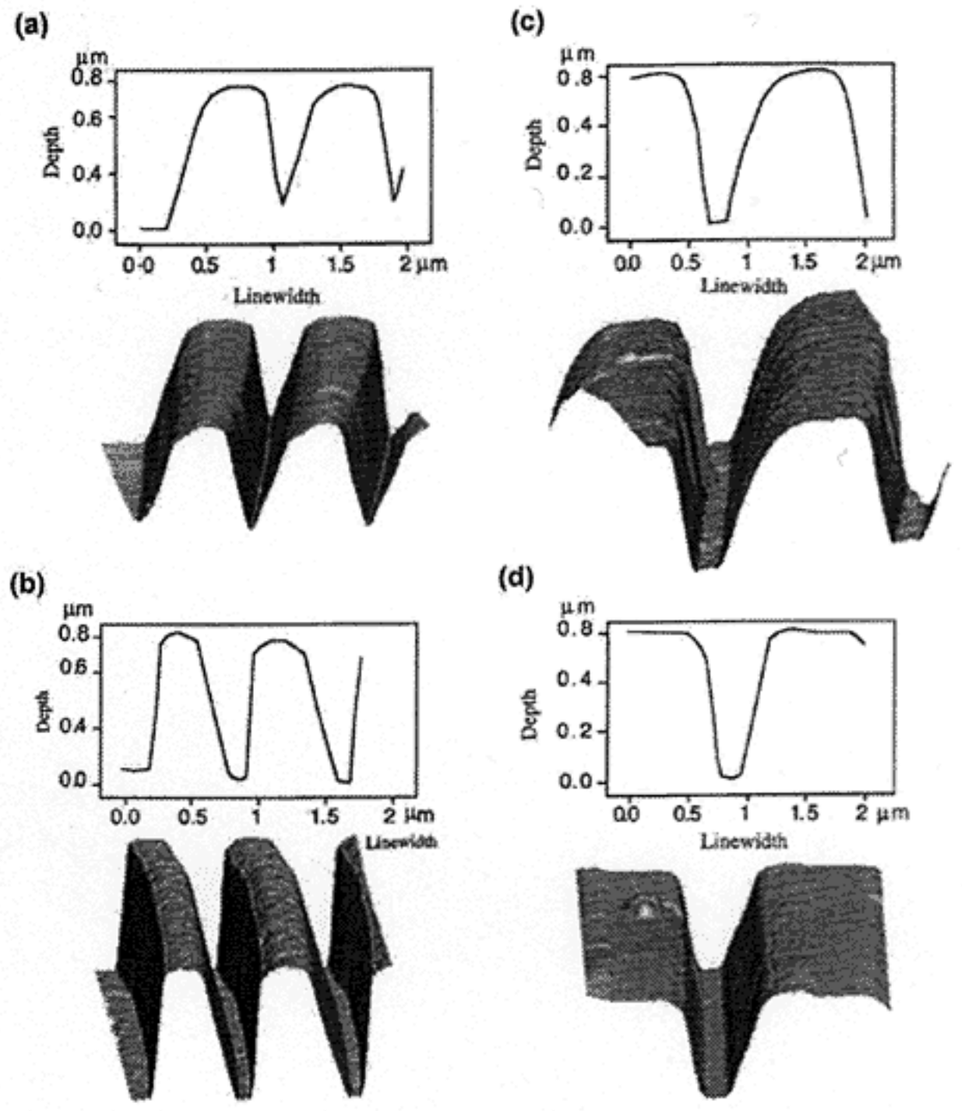

FIG. 2. AFM imaging of nominally 670 nm deep structures of varying linewidth. Here, three-dimensional views and linecuts comparing microfabricated sharp Si tip (NT-MDT SC12 noncontact) and WS_2 nanotube tip are presented. In the left column, a 350 nm linewidth structure is measured by (a) Si microfabricated and (b) WS_2 nanotube tips. (c) and (d) a 600 nm linewidth structure measured with Si microfabricated and WS_2 nanotubes tips, respectively. Note that in case (a), the Si tip cannot reach the bottom of the trench, while the nanotube (b) is able to follow the trench contour.

procedure should give an upper bound for the tip width since the surface features have finite dimensions which augment the image widths. The result of the calculation gave a width of 17 nm for the last 89 nm of the tip length. The image of the replica sidewall gives some measure of the larger tip profile.

The long and narrow geometry of nanotubes results in a relatively weak spring constant in the lateral direction. When imaging deep trenches, attractive forces between tip and sidewall (electrostatic, capillary, etc.) could cause snapping of the nanotube to the wall and resultant instability in scanning. The elastic properties of the nanotube are therefore an important determinant in their usefulness in these measurements. To demonstrate this characteristic, we consider the vdW interaction force (F) between a cylindrical nanotube of radius R and a flat surface (i.e., sidewall of replica) a distance D away over the length L that the nanotube extends into the trench:

$$AR^{1/2}1-/10D^{5/2}, \tag{1}$$

where A is the Hamaker constant, here taken as 5×10^{-20}. The bending force constant (k) of a cylindrical beam fixed at one end is

$$k\cong 2.5R^4E/l^3. \tag{2}$$

Here, R is the nanotube radius and E is the bending modulus for the nanotube, taken as 1 TPa, and l the length of nanotube (note this is generally not equivalent to L).

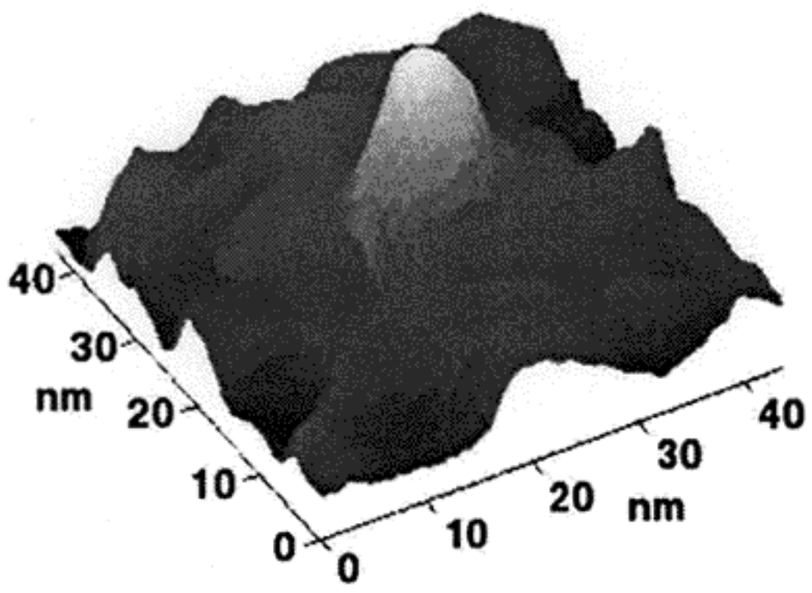

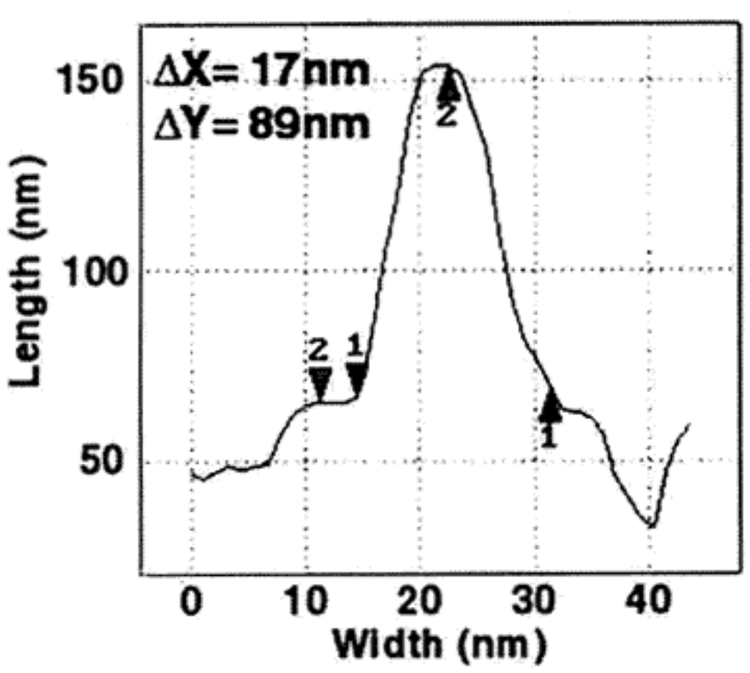

FIG. 3. Blind reconstruction of the shape of the WS_2 nanotube tip which had scanned the "replica" of Fig. 2. The width and the length of the WS_2 nanotube tip is respectively 17 and 89 nm.

Using these formulas, we can calculate the distance between nanotube and sidewall at which the attractive vdW force would cause the nanotube to snap into the sidewall, causing an instability. For a nanotube of 10 nm radius, and 2 μm length, extending 0.5 μm deep into a trench, this distance is 6 nm. Considering that in typical measuring conditions additional forces (capillary, electrostatic) will act to augment this force, the possibility of using nanotube tips for nm-level measurement of steep trenches narrower than 100 nm is fundamentally limited. Equation (2) shows that thicker nanotubes will be substantially more stable, but with concomitant compromise in resolution.

The elastic stiffness coefficients in the basal plane (C_{11}) and along the c axis (C_{33}) of hexagonal 2H–WS_2 and graphite have been reported ($C_{11}=0.15$ TPa for WS_2 and 1.06 TPa for graphite; $C_{33}=60$ GPa for WS_2 and 36.5 GPa for graphite).[6] It is expected that the S–W–S sandwich in the WS_2 layers, will induce an increase of the stiffness in the axial direction of the nanotubes. This could explain the empirical observation that the WS_2 nanotubes appear straight in electron microscope images (Fig. 2 and see also Ref. 1). Also, the present synthesis results in WS_2 nanotubes, which are quite perfect in shape. Both factors are probably responsible for the very good stability and time invariance of the WS_2 nanotube tips.

The axial Young's modulus of carbon nanotubes was estimated using Raman spectroscopy.[7] Concerning the elastic properties of WS_2 nanotubes, no data are yet available as opposed to the tremendous wealth of recent literature for carbon nanotubes.[8–14] Very few studies have been reported on the mechanical properties of other inorganic nanotubes.[11,15] Therefore, further work is necessary to elucidate the mechanical stiffness of the present tips.

The thickness of the WS_2 nanotubes, which are used as AFM tips (20–40 nm), is larger than the usual multiwall carbon nanotubes (5–20 nm^2). The closure of the WS_2 nanotubes at both ends is ascribed to the formation of triangular and rhombohedral defects as is the case for MoS_2 nanoparticles with fullerene-like structure.[16,17] Therefore, their extreme end should be sharper than the one of carbon nanotubes, the latter being only consistent with pentagonal defects.[18] This is seen in the sharp contrast obtained in the Ti asperity surface (not shown) used in the blind reconstruction.

Since the WS_2 nanotubes have similar optical properties to the bulk 2H–WS_2, which is a semiconductor material (indirect gap of 1.3 eV and direct gap of 2.05 eV[19]), the present WS_2 nanotubes can be easily sensitized by visible and infrared light. These WS_2 tips are therefore also very promising for carrying-out photostimulated processes on surfaces.

The authors thank Mr. Van der Wal from Philips Electron Optics B.V. (Eindhoven) and for the SEM picture taken on a XL30-ESEM FEG instrument. This work was supported by a grant from the Israeli Ministry of Science (Tashtiot) and from Applied Materials, Inc. They are grateful to Dr. Avner Karpol and Nadav Haas of this company for providing the "replica" which has been used for the present study.

[1] A. Rothschild, G. L. Frey, M. Homyonfer, M. Rappaport, and R. Tenne, Materials Res. Innovations **3**, 145 (1999).
[2] H. Dai, J. H. Hafner, A. G. Rinzler, D. T. Colbert, and R. E. Smalley, Nature (London) **384**, 147 (1996). See also, J. H. Hafner, "Nanotube tips for SFM," http://cnst.rice.edu/mount/html.
[3] J. H. Hafner, C. L. Cheung, and C. M. Lieber, Nature (London) **398**, 761 (1999).
[4] K. L. Westra and D. J. Thomson, J. Vac. Sci. Technol. B **13**, 344 (1995), obtainable from General Microdevices, Edmonton, Alberta, Canada.
[5] Blind reconstruction algorithm developed by A. Efimov, obtainable at http://www.siliconmdt.com.
[6] C. Sourisseau, M. Fouassier, M. Alba, A. Ghorayeb, and O. Gorochov, Mater. Sci. Eng., B **3**, 119 (1989).
[7] O. Lourie and H. D. Wagner, J. Mater. Res. **13**, 2418 (1998).
[8] M. M. Treacy, T. W. Ebbesen, and J. M. Gibson, Nature (London) **381**, 678 (1996).
[9] E. W. Wong, P. E. Sheelan, and C. M. Lieber, Science **277**, 1971 (1997).
[10] J. P. Liu, Phys. Rev. Lett. **79**, 1297 (1997).
[11] E. Hernandez, C. Goze, P. Bernier, and A. Rubio, Appl. Phys. A: Mater. Sci. Process. **68**, 287 (1999).
[12] A. Krishnan, E. Dujardin, T. W. Ebbesen, P. N. Yianilos, and M. M. J. Treacy, Phys. Rev. B **58**, 14013 (1998).
[13] J. P. Salvetat, G. Andrew, D. Briggs, J. M. Bonard, R. R. Bacsa, A. J. Kulik, T. Stockli, N. A. Burnham, and L. Forro, Phys. Rev. Lett. **82**, 944 (1999).
[14] B. I. Yacobson, C. J. Brabec, and J. Bernhole, Phys. Rev. Lett. **76**, 2511 (1996).
[15] N. G. Chopra and A. Zettl, Solid State Commun. **105**, 297 (1998).
[16] L. Margulis, G. Salitra, M. Talianker, and R. Tenne, Nature (London) **365**, 113 (1993).
[17] P. A. Parilla, A. C. Dillon, K. M. Jones, G. Riker, D. L. Schulz, D. S. Ginley, and M. J. Heben, Nature (London) **397**, 114 (1999).
[18] P. M. Ajayan, in *Carbon Nanotubes: Preparation and Properties*, edited by T. W. Ebbesen (CRC Press, Boca Raton, Florida, 1997), Chap. 3, p. 111.
[19] C. Ballif, P. E. Regula, M. Remskar, R. Sanjinés, and F. Lévy, Appl. Phys. A: Solids Surf. **62**, 543 (1996).